Heliyon 10 (2024) e35636

Contents lists available at ScienceDirect

Heliyon

journal homepage: www.cell.com/heliyon

Research article

Therapeutic effect of oral insulin-chitosan nanobeads pectin-dextrin shell on streptozotocin-diabetic male albino rats

Hanaa Ramadan [a], Nadia Moustafa [a], Rasha Rashad Ahmed [a], Ahmed A.G. El-Shahawy [b], Zienab E. Eldin [b], Suhailah S. Al-Jameel [c,d], Kamal Adel Amin [c,d], Osama M. Ahmed [e], Manal Abdul-Hamid [a,*]

[a] Cell Biology, Histology and Genetics Division, Department of Zoology, Faculty of Science, Beni-Suef University, P.O. Box 62521, Beni-Suef, Egypt
[b] Materials Science and Nanotechnology Department, Faculty of Postgraduate Studies for Advanced Sciences (PSAS), Beni-Suef University, 62521 Beni-Suef 12827, Egypt
[c] Department of Chemistry, College of Science, Imam Abdulrahman Bin Faisal University, Dammam, Saudi Arabia
[d] Basic and Applied Scientific Research Center, Imam Abdulrahman Bin Faisal University, Dammam, Saudi Arabia
[e] Physiology Division, Zoology Department, Faculty of Science, Beni-Suef University, P.O. Box 62521, Beni-Suef, Egypt

ARTICLE INFO

Keywords:
Diabetes
Nanoparticles
Insulin-loaded chitosan nanobeads
INS-CsNBs-PD
NF-κB P65
SIRT-1
Oxidative stress biomarkers
Histopathology

ABSTRACT

The current study inspects the therapeutic effects of orally ingested insulin-loaded chitosan nanobeads (INS-CsNBs) with a pectin-dextrin (PD) coating on streptozotocin (STZ)-induced diabetes in Wistar rats. The study also assessed antioxidant effects in pancreatic tissue homogenate, insulin, C-peptide, and inflammatory markers interleukin-1 beta and interleukin-6 (IL-1β and IL-6) in serum. Additionally, histopathological and immunohistochemical examination of insulin granules, oxidative stress, nuclear factor kappa B (NF-κB P65), and sirtuin-1 (SIRT-1) protein detection, as well as gene expression of nuclear factor erythroid 2–related factor 2 (Nrf2), heme oxygenase-1 (HO-1), B-cell lymphoma 2 (Bcl2), and Bcl-2-associated X protein (Bax) in pancreatic tissue were investigated. After induction of diabetes with STZ, rats were allocated into 6 groups: the normal control (C), the diabetic control (D), and the diabetic groups treated with INS-CsNBs coated with PD shell (50 IU/kg) (NF), free oral insulin (10 IU/kg) (FO), CsNBs-PD shell (50 IU/kg) (NB), and subcutaneous insulin (10 IU/kg) (Sc). The rats were treated daily for four weeks. Treatment of diabetic rats with INS-CsNBs coated with PD shell resulted in a significant improvement in blood glucose levels, elevated antioxidant activities, decreased NF-κB P65, IL-1β, and IL-6 levels, upregulated Nrf-2 and HO-1, in addition to a marked improvement in the histological architecture and integrity compared to the diabetic group. The effects of oral INS-CsNBs administration were comparable to those of subcutaneous insulin. In conclusion, oral administration of INS-loaded Cs-NBs with a pectin-dextrin shell demonstrated an ameliorative effect on STZ-induced diabetes, avoiding the drawbacks of subcutaneous insulin.

* Corresponding author. Histology and Cell Biology Division, Zoology Department, Faculty of Science, Beni-Suef University, Egypt, Salah Salem St., 62521, Beni-Suef, Egypt.
E-mail addresses: ssaljameel@iau.edu.sa (S.S. Al-Jameel), kaothman@iau.edu.sa (K.A. Amin), medo_bio@yahoo.com, manal.mohamed3@science.bsu.edu.eg (M. Abdul-Hamid).

https://doi.org/10.1016/j.heliyon.2024.e35636
Received 25 February 2024; Received in revised form 31 July 2024; Accepted 1 August 2024
Available online 6 August 2024

1. Introduction

The β-cells in islets of the diabetic pancreas undergo immune-mediated malfunction, necrosis, and apoptosis, which causes insufficient or nonexistent insulin production and prolonged hyperglycemia [1,2]. The production of reactive oxygen species (ROS) and the alkylation of deoxyribonucleic acid (DNA) are two mechanisms by which streptozotocin (STZ) damages pancreatic β-cells [3].

Abbreviations

NF-κB p65	Nuclear factor kappa-light-chain-enhancer of activated B cells
SIRT1	Sirtuin-1
HO-1	Heme oxygenase-1
Nrf2	Nuclear factor erythroid 2–related factor 2
Bcl2	B-cell lymphoma 2
Bax	Bcl-2-associated X protein
GAPDH	Glyceraldehyde-3-phosphate dehydrogenase

The formation of ROS has also been linked to hyperglycemia, hence oxidative stress is currently proposed as the mechanism explaining diabetes and diabetic complications [4]. The function of T cells is altered, and they release numerous cytokines that cause inflammation in the pancreatic islets, damaging the β-cells and impairing their ability to produce insulin [5,6]. High levels of glucose and free fatty acids exacerbate oxidative cellular damage and yield detrimental effects by causing the production of free radicals and weakening antioxidant responses [7]. NF-κB p65 is a transcription factor that regulates a significant number of genes involved in apoptosis, immune response, inflammation, and cellular proliferation. It also markedly influences cellular responses to stress and free radicals [8]. SIRT-1 plays a crucial role in various processes, including cell division, differentiation, senescence, gene regulation, mitochondrial biogenesis, fatty acid oxidation, apoptosis, autophagy, and metabolic control of the cell [9]. HO-1, a cyto-defensive and antioxidant gene, is upregulated by the transcription factor Nrf2, which provides protection against excessive ROS and oxidative stress [10].

Currently, the main treatment for Type 1 diabetes (T1DM) is exogenous insulin replacement therapy. Inadequate insulin dosing is a critical limitation that often leads to complications from hyperglycemia or hypoglycemia. Insulin injections may lead to hypoglycemia, coma, and ketosis, as they cannot precisely regulate blood glucose levels or prevent diabetes-related complications. Exogenous insulin cannot maintain blood glucose levels within the same range as endogenous insulin produced by pancreatic β-cells [11]. Recent studies have concentrated on enhancing the bioavailability and absorption of orally administered insulin [12].

Natural nano-carriers, especially polysaccharides, exhibit high levels of biocompatibility and biodegradability. Furthermore, they provide enhanced safety, improved storage conditions, and greater physiological stability. They can increase the stability of insulin by reducing its enzymatic and hydrolytic degradation [13]. Chitosan (Cs) is an effective natural polysaccharide known for its abundant availability, biocompatibility, biodegradability, non-toxicity, low cost, and strong mucoadhesive properties [14]. Cs-insulin nanoparticles enhance insulin's penetration rate into the bloodstream via paracellular pathways and prolong its residence time in the small intestine [15]. Pectin, a biocompatible polysaccharide, possesses potent hypoglycemic, antioxidant, and immunomodulatory properties [16]. Pectin nanoparticles have improved blood glucose and lipid levels, reduced insulin resistance, liver glycogen content, and glucose tolerance, and ameliorated the conditions and consequences of diabetes [17]. Unlike other polysaccharides, dextran is resistant to digestion by standard amylases, including salivary and malt amylase. It can only be depolymerized by dextranase in the lumen of the kidney, liver, spleen, and large intestine. Consequently, dextran-based drug delivery systems can protect drug molecules from enzymatic and chemical degradation in the stomach and small intestine, enhancing intestinal epithelial uptake and oral bioavailability [18].

The quest for alternative methods to subcutaneous insulin injections, aimed at minimizing the histopathological damage caused by diabetes, has become crucial. This study focuses on developing and evaluating orally administered insulin-loaded chitosan nanobeads with a pectin-dextrin coating (INS-CsNBs PD shell) for managing streptozotocin (STZ)-induced diabetes in Wistar rats. The primary research question investigates whether this innovative formula can enhance blood glucose levels. Our hypothesis is that the INS-CsNBs PD shell will significantly enhance glucose regulation. Additionally, we will evaluate antioxidant activity changes, hypothesizing that our formula will increase these activities. Moreover, the study aims to assess the impact on pancreatic histology, with a particular focus on preserving beta cells and preventing their destruction. This research fills a critical gap in developing non-invasive insulin delivery systems that offer protective benefits to pancreatic tissue.

2. Materials and methods

2.1. Materials

STZ, Cs with medium molecular weight, dextrin from corn (D2006), pectin (P9135 25G 100G), and sodium tri-polyphosphate (TPP) were purchased from Sigma-Aldrich Co., MO, USA. Commercial insulin (Novo Nordisk, 100 IU/ml) was also acquired. Glacial acetic acid, sodium hydroxide, and all other reagents of analytical grade were obtained from commercial sources: the kits for determination of malondialdehyde (MDA) and catalase (CAT), superoxide dismutase (SOD), glutathione peroxidase (GPx), and reduced glutathione (GSH) were purchased from BioDiagnostic CO, Dokki, Giza, Egypt.

2.2. Synthesis of INS-loaded CsNBs coated with PD shell

An improved ionic gelation technique was used to create the INS-CsNBs-PD shell [19]. Briefly, the concentration of chitosan (0.3 %, w/v) in DW containing 1 % acetic acid, pH 4.8, and the chitosan/TPP ratio of 4:1 has been investigated. Nanoparticles were formed following the drop-wise addition of TPP solution to the chitosan solution, with magnetic stirring for 30 min at 1000 r.p.m. Subsequently, 0.1g of dextrin was dispersed in 10 mL of deionized water (1.0 % w/v). The mixture was completely gelatinized in a boiling water bath before being cooled to room temperature. Insulin (500 μg/ml) was then added dropwise to the dextrin solution, followed by magnetic stirring at 1000 r/min for 1 h. Pectin (4 % w/v) was subsequently incorporated using a high-speed homogenizer into the chitosan-dextrin-insulin mixture, which was then maintained at 4 °C for 48 h. Finally, the solution was centrifuged in a cooling centrifuge and lyophilized to yield the powder.

2.3. Characterizations

2.3.1. Morphological study

The surface morphology and particle size of the prepared INS-loaded CsNBs with a PD coating were investigated using a high-resolution transmission electron microscope (HR-TEM) with a JEM 1400 (Japan) operated at 300 kV. A drop of the prepared formula was placed on a film-coated copper grid, stained with a 2 % (w/v) aqueous solution of phosphor-tungstic acid, and allowed to dry to enhance contrast. The sample was then examined by HR-TEM. Additionally, a field emission scanning electron microscope (FESEM) using a Philips-XL30 device (Netherlands) equipped with energy-dispersive X-ray microanalysis hardware was used. The samples were prepared by dispersing the specimens in deionized water and diluting them to a 1:5 (v/v) ratio at room temperature.

2.3.2. Determination of the entrapment efficiency (EE) and drug loading (DL) of insulin onto CsNBs-PD shell nanoparticles

The entrapment efficiency and drug loading of insulin onto CsNBs-PD shell nanoparticles were assessed by centrifuging the samples at 16,000 rpm at 4 °C for 30 min to separate the supernatant containing free insulin. The amount of free insulin in both centrifuged and non-centrifuged INS-CsNBs-PD shell solutions was quantified using HPLC analysis. All measurements were performed in triplicate (n = 3). The entrapment efficiency (EE%) and drug loading (DL%) of insulin were calculated as follows:

(EE %) = [Amount of insulin originally taken - Amount of insulin in supernatant/ Amount of insulin originally taken *100]. Eq 1

(DL %) = [Amount of insulin originally taken /amount of CsNBs-PD shell loaded insulin*100]. Eq 2

2.4. In-vivo study

2.4.1. Experimental design

Male Wistar albino rats (n = 36) with an average body weight of 100–140g were acquired from VACSERA (Cairo, Egypt). In the animal house, rats were housed in clean, aerated cages with access to water and food, under optimal conditions with a humidity of 45

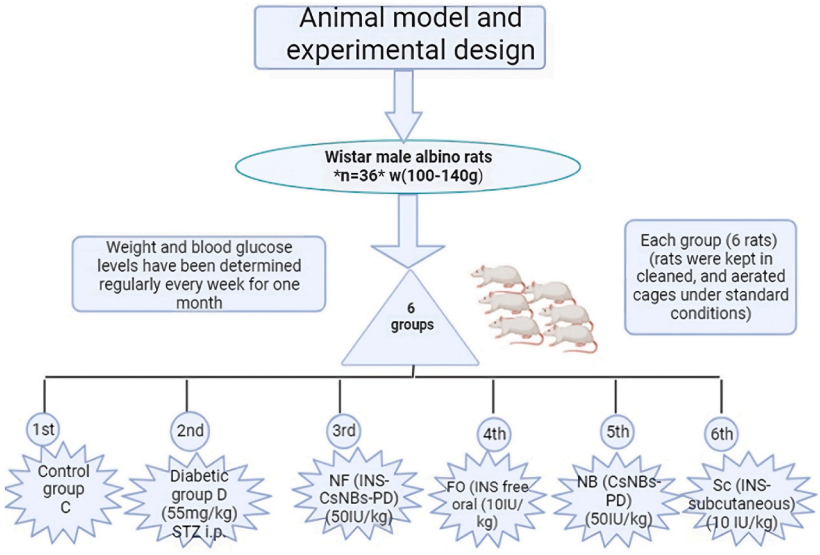

Fig. 1. A schematic diagram of the animal model and experimental design. C: the control group; D is the diabetic group; NF: oral nano-formula (INS-CsNBs-PD); FO: oral free insulin; NB is oral nano-formula (Nanobeads Blank Control); Sc: is subcutaneous insulin.

± 5 % and a temperature of 30 ± 4 °C, and a regular 12-h dark/light cycle. Before the experiment, animals were acclimated for one week, consuming only water and a basal diet consisting of 50–52 % carbohydrates, 17 % protein, 5.0 % fat, and other nutritional sources. The experiment was conducted in accordance with the animal ethics guidelines of the Institutional Animal Care and Use Committee at Beni-Suef University (IACUC Approval Number: BSU-FS-021-128).

2.4.2. Induction of type1 diabetes mellitus (DM)

In this study, overnight fasted albino rats were intraperitoneally (i.p.) injected with a single dose (55 mg/kg) of STZ, which was dissolved in a 0.1 M citrate buffer solution (pH = 4.5) [20]. To prevent hypoglycemic shock, STZ-induced diabetic rats were supplemented with 10 % glucose in their drinking water after 4 h of induction. Diabetes mellitus (DM) was confirmed four days later by measuring blood glucose levels (BGL) after overnight fasting. Fasting and postprandial blood glucose levels were measured using the CERA-CHECKTM 1070, a Korean glucometer. Rats with fasting blood glucose levels above 180 mg/dl were considered diabetic. Weight and blood glucose levels were regularly determined every week for one month.

2.4.3. Animal grouping

Fig. 1 illustrates a schematic diagram of the animal model and experimental design. Wistar male experimental albino rats were divided into six groups, with each group consisting of six rats. The first group is the normal control © treated only with sodium citrate buffer (0.1 M, pH = 4.5). The second group (D) is the control diabetic group injected with a single dose of STZ (55 mg/kg) [20]. The third group (NF) includes diabetic rats that were orally administered INS-loaded CsNBs coated with a PD shell in HCl (0.025M) at a dose of 50 IU/kg, depending on the encapsulation efficiency of insulin [21]. The fourth group (FO) consists of diabetic rats treated with free oral insulin (10 IU/kg) to investigate the oral administration route. The fifth group (NB) is considered a blank control group treated orally with only nanoparticles (CsNBs-PD shell in HCl (0.025M)) at a dose of 50 IU/kg. The sixth group (Sc) is a diabetic group that was subcutaneously injected with insulin (10 IU/kg) [22]. After one week of STZ injection, rats received daily treatments for 4 weeks.

2.4.4. Blood sampling and ELISA assay

Every week during the experiment and the day before sacrifice, blood was collected from the lateral veins of the rat tail to measure fasting and postprandial blood glucose levels (BGLs) using the CERA-CHECK™ 1070 glucometer, which has a maximum measuring capacity of 600 mg/dl. At the end of the experiment, all rats were sacrificed, and blood samples were immediately collected from the inferior vena cava into vacuum blood collection tubes. These tubes were then centrifuged at 3000 rpm for 10 min to separate the sera. The sera samples (n = 6) were stored at −20 °C until analysis. Serum insulin and C-peptide levels were estimated using the ultra-sensitive rat insulin and C-peptide ELISA kits (Crystal Chem, Inc., USA) according to the manufacturer's instructions. Interleukin-1β (IL-1β) and interleukin-6 (IL-6) levels were estimated by enzyme-linked immunosorbent assay kits purchased from Cloud-Clone Corp (CCC, USA) following the manual instructions. Protein content was measured using Kruger's method with the Genei, Bangalore, protein estimation kit [23].

2.4.5. Preparation of tissue homogenate and oxidative stress determination

We excised pancreatic organs, and samples were dissected and subsequently thawed at −70 °C following a rinse in liquid nitrogen. Pieces of pancreatic tissues from all groups were weighed and homogenized using a homogenizer to achieve a 10 % w/v concentration with ice-cold phosphate buffer (PBS/pH = 7.4) [24]. Tissue homogenates were centrifuged at 4000 rpm for 10 min. The supernatants were stored at −20 °C for subsequent determination of oxidative stress markers. Samples from each group (n = 6) were analyzed. MDA levels were measured as a biomarker of lipid peroxidation [25]. Antioxidant enzyme levels, including CAT, SOD, GST, GPx, and GSH, were also measured [26].

2.4.6. Histological examination

By decapitation under light anesthesia, all rats were sacrificed after the fourth week. Immediately afterward, pancreas samples were dissected and sectioned. Pieces of each pancreatic tissue were placed in 10 % neutral buffered formalin for one day to fix the tissues. Water was removed from the fixed tissues by progressively increasing the concentration of alcohol, preparing them for paraffin embedding. Before embedding, pancreatic tissues were cleared by replacing alcohol with xylene. Subsequently, the tissues were embedded in paraffin wax at 60 °C. Paraffin-embedded pancreatic blocks were then sliced into thin sections of approximately 4 μm using a microtome. De-paraffinized tissue sections (n = 6) were stained with hematoxylin and eosin (H&E) for histological examination [27].

2.4.7. Immunohistochemistry and morphometric analysis

Insulin granules were detected in the pancreatic islets using immunohistochemical staining [28]. Briefly, 4 μm thick sections of paraffinized and rehydrated pancreatic tissues were mounted on specific slides (positively charged). The sections were washed with 0.1 M phosphate-buffered saline (PBS). Following the manufacturer's instructions, the immunohistochemical process (IHC) was applied to these slides (n = 6) using the Avidin-Biotin detection system (Ventana, Tucson, AZ, USA). To prevent non-specific binding due to endogenous peroxidase, non-specific binding was prevented by incubating the sections in 3 % H2O2 for 10 min, boiling in citrate buffer, pH 6, and blocking with a protein block. Primary anti-insulin antibodies (ICBTACLS), biotin, eBioscience™, acquired from Thermo Scientific, USA, were applied to the tissue sections for insulin detection.

The area percentage of insulin immune-expression reaction was measured using ImageJ software analyzer (Wayne Rasband, NIH, Bethesda, MD, USA) at a magnification of × 400 [29]. Five distinct non-overlapping immune-stained fields were examined in pancreatic tissues of each animal. Data are expressed as the mean ± SE.*2.4.8.*

2.4.8. Quantitative real-time polymerase chain reaction (qRT-PCR)

Gene expression or mRNA abundance of Bcl2-associated X apoptotic activator (Bax), anti-apoptotic mediator Bcl2 (B-cell lymphoma 2), Nrf2, and HO-1 were studied by qRT-PCR. RNA was extracted from frozen pancreatic samples (−80 °C) (n = 6) using a nucleic acid extraction kit (NucleoSpin® REF. 740901.250) purchased from Macherey-Nagel GmbH & Co. KG, Germany. The concentrations and purity (A260/A280 ratio) of the mRNA samples were measured at 260 nm using spectrophotometry (dual wavelength Beckman spectrophotometer, USA) [30]. Reverse transcriptase catalyzed the conversion of RNA into complementary DNA (cDNA) from the RNA samples, which were then amplified using SYBRTM Green (SensiFAST™) PCR Master Mix (Thermo Scientific, USA) [31]. The primer sets were listed (Table 1). The prepared reaction mixtures were subjected to real-time PCR (StepOne Applied Biosystem, Foster City, USA). Data analysis was performed using the (2ˆ{-\Delta\Delta Ct}) method, and the expression levels of each target gene were normalized to GAPDH (the reference gene) and expressed as a percentage of the control [32].

2.4.9. Western blot (WB) assay

Total proteins from homogenized pancreatic samples (n = 6) were extracted using the Ready PrepTM protein extraction kit (total protein) provided by Bio-Rad Inc (Catalog #163–2086), following the manufacturer's instructions. The Bradford Protein Assay Kit (SK3041) from Bio Basic Inc. (Markham Ontario L3R 8T4 Canada) was used for quantitative protein analysis. A 20 μg protein concentration from each sample was separated by SDS polyacrylamide gel electrophoresis (SDS-PAGE) using the TGX Stain-Free™ Fast Cast™ Acrylamide Kit from Bio-Rad Laboratories Inc (Cat # 161–0181). Proteins were transferred from the gel to a polyvinylidene difluoride (PVDF) membrane and blocked in tris-buffered saline with Tween 20 (TBST) buffer and 3 % bovine serum albumin (BSA) to prevent non-specific binding of antibodies [38]. The protein of interest was detected (in triplicate) by incubating with the primary antibody, followed by secondary antibody incubation. Primary antibodies used for Western blotting of NFκB p65 and SIRT1 were NF-κB p65 (F-6): sc-8008, and anti-SIRT1 (B-7): sc-74465 antibodies. Protein levels were normalized to β-actin, which was used as the loading control. Anti-β-Actin [(C-2): sc-8432] was provided by Santa Cruz Biotechnology, Inc., CA 95060, USA [39]. The electrogenerated chemiluminescence (ECL) detection system from Pierce, Rockford, IL, was used to visualize the immunoreactive bands. The chemiluminescent substrate was Clarity-TM Western ECL substrate (Bio-Rad cat#170–5060).

2.5. Statistical studies

All data were reported and presented as the mean ± standard error (SE). The statistical software IBM SPSS Statistics 17 (NY, USA) was used for data analysis using one-way analysis of variance (ANOVA) followed by a post hoc test. Differences between groups were considered statistically significant if the p-value was less than or equal to 0.05 ($P < 0.05$).

Along with statistical analyses, individual data were shown as scattered dots on graphs.

3. Results

3.1. Morphological studies (HRTEM and FESEM)

Fig. 2 demonstrates high-resolution transmission electron micrographs of INS-CsNBs-PD nanoparticles (NPs). HRTEM images revealed roughly spherical particles with an average size of 92 nm. Field Emission Scanning Electron Microscopy (FESEM) images (Fig. 3) showed spherical particles with smooth surfaces. These particles exhibit relatively uniform size and shape. The mean diameter was approximately 100 nm. There was no notable difference in the particle size between HRTEM and FESEM images.

Table 1
Primer sequence (Forward and Reverse) for qRT-PCR.

Gene	Gene accession number	Primer sequence (5′→3′)	Reference
Bax	U32098.1	F: CCTGAGCTGACCTTGGAGCA R: GGTGGTTGCCCTTTTCTACT	[33]
Bcl2	NM_016993.1	F: TGATAACCGGGAGATCGTGA R: AAAGCACATCCAATAAAAAGC	[34]
Nrf2	NM_031789.2	F: TCCCAAACAAGATGCCTTGT R: AGAGGCCACACTGACAGAGA	[35]
HO-1	NM_012580	F: CACCAGCCACACAGCACTAC R: CACCCACCCCTCAAAAGACA	[36]
GAPDH	NM_017008.4	F: GGATACTGAGAGCAAGAGAGA R: TTATGGGGTCTGGGATGGAA	[37]

Bax, BCL2 Associated X, Apoptosis Regulator: Bcl2, B-cell lymphoma 2: Nrf2, nuclear factor, erythroid 2: HO-1, Heme oxygenase-1: GAPDH, glyceraldehyde-3-phosphate dehydrogenase.

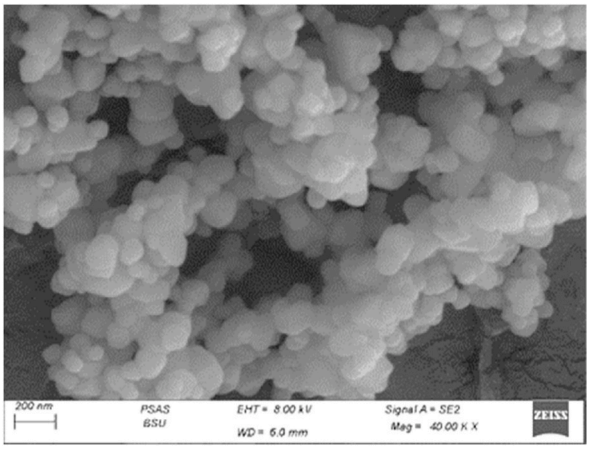

Fig. 2. FESEM image of prepared nano-formula (INS-CsNBs-PD shell.

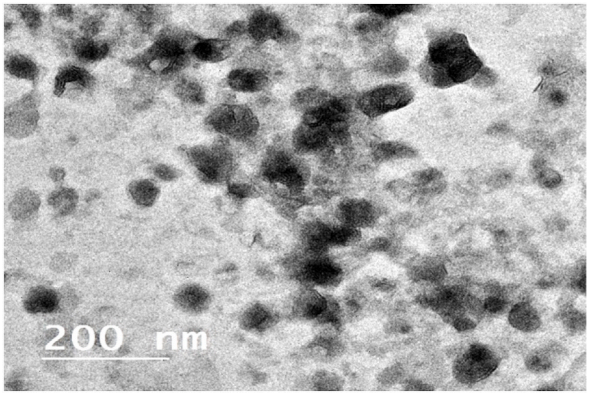

Fig. 3. HR-TEM photograph of prepared nano-formula (INS-CsNBs-PD shell).

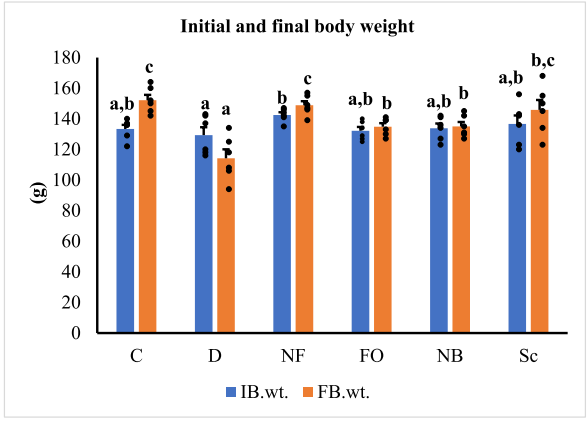

Fig. 4. The initial (IB.wt.) and final (FB.wt.) body weights. Results are presented as mean ± SEM where n = 6. C: Control rats, D: Diabetic control rats, NF: Diabetic rats treated with the oral formula (INS-CsNBs-PD shell), FO: Diabetic rats treated with free oral insulin, NB: Diabetic rats treated with the blank oral formula (CsNBs-PD shell) and Sc: Diabetic rats injected with INS subcutaneously. $^{b,c}p < 0.05$ significantly different from the diabetic group and $^{c}p < 0.05$ and $^{a,b}p < 0.05$ significantly different from the control group for initial ($F = 1.480$, $P < 0.05$) and final ($F = 10.592$, $P < 0.05$) body weights respectively. Groups with the same superscript letter did not represent any significant differences.

3.2. Entrapment efficiency and drug loading of INS-CsNBs-PD shell

Based on Equations (1) and (2), the encapsulation efficiency of INS-CsNBs-PD shell nanoparticles was determined to be (69.3 ± 2.75) %, and the drug loading was (26.28 ± 0.56) % (n = 3). These results confirm the successful preparation of INS-CsNBs-PD shell nanoparticles.

3.3. Body weight and BGLs

Fig. 4 displays the initial and final body weights of various treatment groups. Initially, there was no discernible difference in the body weights of the rats across all groups, but by the end of the study, the body weight of the untreated diabetic rats significantly decreased ($p < 0.05$) compared to the control group. The study established that after four weeks of treatment, both the oral INS-CsNBs-PD shell and injected insulin significantly increased the body weight of diabetic rats ($p < 0.05$). However, there was no statistically significant difference observed between these two treatments. The use of chitosan nanoparticles loaded with insulin and coated with a protective layer resulted in an improvement in the body weight of rats with STZ-induced diabetes.

Fasting and postprandial blood glucose levels were illustrated (Fig. 5). Four weeks after the STZ injection, the untreated diabetic group had higher fasting and postprandial blood glucose levels compared to the healthy control group ($P < 0.05$). Nevertheless, the oral administration of insulin-loaded chitosan nanobeads with a pectin-dextrin shell, similar to subcutaneous insulin injections, significantly reduced FBS and PBS levels compared to the untreated diabetic group ($P < 0.05$). Compared to insulin injections, the insulin-loaded CsNBs-PD shell demonstrated a greater potential to lower blood glucose levels. Studies indicated that, compared to rats given oral insulin and subcutaneous insulin injections, the insulin-loaded CsNPs significantly lowered blood glucose levels in a diabetic rat model. After oral administration of the Cs-NBs-PD shell nano-formula, fasting and postprandial blood glucose levels were noticeably reduced due to the incorporation of pectin and chitosan ($P < 0.05$).

3.4. Histopathological examinations

Normal pancreatic tissues, with well-preserved cytoplasm and nuclei, as well as pancreatic acini with an oval or rounded appearance, were visible in the sections. The pancreatic acini had relatively few connective tissue septa between the pyramidal cells lining them, which were organized around a small acinar lumen and contained zymogen granules in their cytoplasm. The islets of Langerhans appeared as non-encapsulated, pale-colored round or oval clusters, composed of cell clusters arranged in irregular, branching, and anastomosing cords separated by blood capillaries (Fig. 6a). Compared to the control group, STZ treatment in the diabetic group significantly altered the pancreatic islets, primarily at their centers, showing cellular degenerations. The pancreatic islets generally appeared smaller and less numerous, with complete degeneration observed in some sections. Damaged cells with cytoplasmic vacuolation, necrotic changes, and pyknotic nuclei were observed (Fig. 6b). Other pancreatic islets had shrunken cells with acidophilic, vacuolated cytoplasm and congested blood vessels (Fig. 6c). The significant alterations observed in the diabetic rats improved markedly after oral administration of the INS-CsNBs-PD shell nano-formula. Numerous islets of various sizes were observed, revealing islets with improved degenerative alterations and a small number of β-cell regeneration (Fig. 6d). The pancreatic islets of diabetic rats treated with free oral insulin showed decreased volume and congested blood capillaries, with minimal improvement in oxidative stress markers (Fig. 6e). In diabetic rats treated with subcutaneous insulin, the pancreatic islet structure was restored, with only a few hyperchromatic nuclei detectable and a significant increase in islet size (Fig. 6g).

3.5. Immunohistochemistry (IHC) and morphometric study of insulin granules

The core region of the islets was occupied by the β-cells, or insulin-secreting cells, which constituted the majority of the islet cell

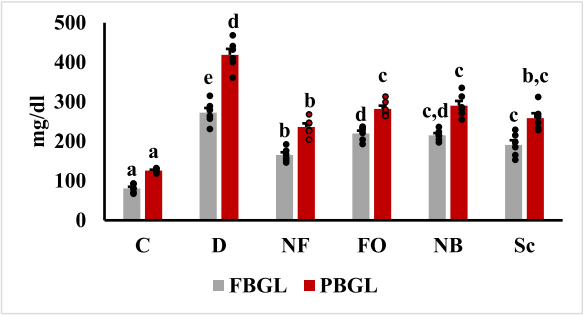

Fig. 5. Fasting and postprandial blood glucose levels after treatment. Results was presented as mean ± SEM, where n = 6. FBGL: fasting blood glucose levels ($F = 58.298$, $P < 0.05$); PBGL: final postprandial blood glucose levels ($F = 78.990$, $P < 0.05$). $^{a,b,c}p < 0.05$ significantly different from the diabetic group and $^{b,c,d,e}p < 0.05$ significantly different from the control group. Groups with the same superscript letter did not represent any significant differences.

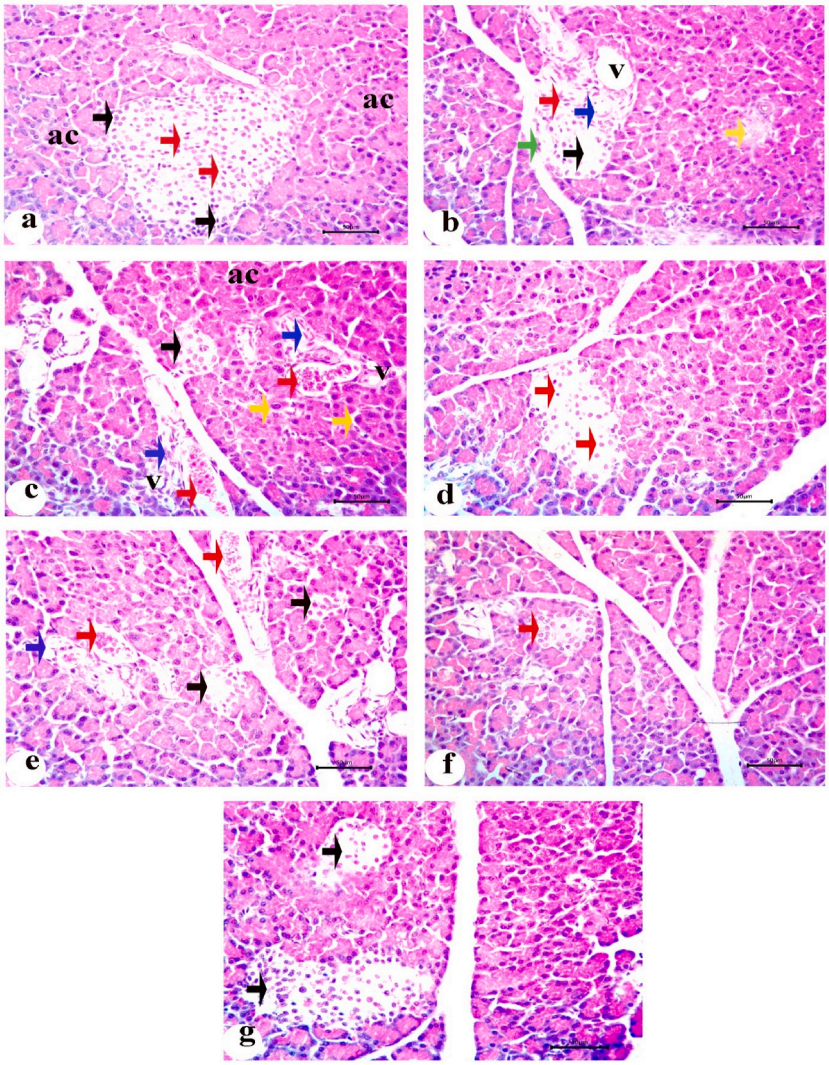

Fig. 6. Photomicrographs of the pancreatic sections stained with H&E. a) The control group (C) showing normal pancreatic acini (ac), islet of Langerhans contains alpha cells on the peripheral side with dark, small peripheral nuclei (black arrows) and cords of β-cells with light and large nuclei (red arrows); b) Untreated diabetic group (D) revealing islets of Langerhans with cytoplasmic vacuolation (V), degeneration (black arrow), pyknosis (red arrow), necrosis of β-cells (blue arrow) and mitotic figure (green arrow). There are completely shrunken and degenerated islet (yellow arrow); c) Another pancreatic section of diabetic group (D) revealed karyomegaly of acinar cells (yellow arrows), apoptosis (blue arrows) and small shrunken islet (black arrow) in addition to congestion (red arrows); d) Pancreatic section of treated group orally with INS-CsNBs-PD shell (F) displaying islet with regeneration of small number of β-cells and improving of degenerative changes (red arrows); e) Pancreatic section from the diabetic group treated with free insulin via oral administration (FO) presenting shrinkage in islets with degeneration (black arrows), congestion (red arrows) and cytoplasmic vacuolation (blue arrow); f) Pancreatic section of diabetic group treated orally with CsNBs-PD shell (NB) showing small islet without degenerative effect of these nanoparticles (red arrow); g.) The section of treated group injected with subcutaneous insulin (Sc) exhibiting of islets with ameliorative effect and regeneration of β-cells with considerable rise in islet volume (black arrows). (Scale bar = 50 μm) (n = 6). (For interpretation of the references to color in this figure legend, the reader is referred to the Web version of this article.)

population. The β-cells were identified by dark brown cytoplasmic granules, a hallmark of normal positive insulin expression, as β-cells treated with anti-insulin antibodies exhibited an effective positive reaction (Fig. 7a). The immunological response to anti-insulin antibodies was significantly reduced due to the decrease in insulin-positive β-cells and the alteration of their distribution (Fig. 7b). There was an insignificant immunohistochemical expression of insulin following the oral administration of the INS-CsNBs-PD shell formula, which was associated with a limited number of β-cells (Fig. 7c). Rats given free oral insulin had tiny islets, a substantial loss of β-cells, and an immunohistochemical insulin response similar to that of the control diabetic group (Fig. 7d). Moreover, the oral administration of CsNBs-PD shell nanoparticles resulted in a significant reduction of insulin expression in pancreatic sections due to the presence of few normal β-cells (Fig. 7e). Sections from the pancreas of the diabetic group that received subcutaneous insulin injections displayed a marked increase in β-cells expressing insulin and had normal density compared to the diabetic group (Fig. 7f).

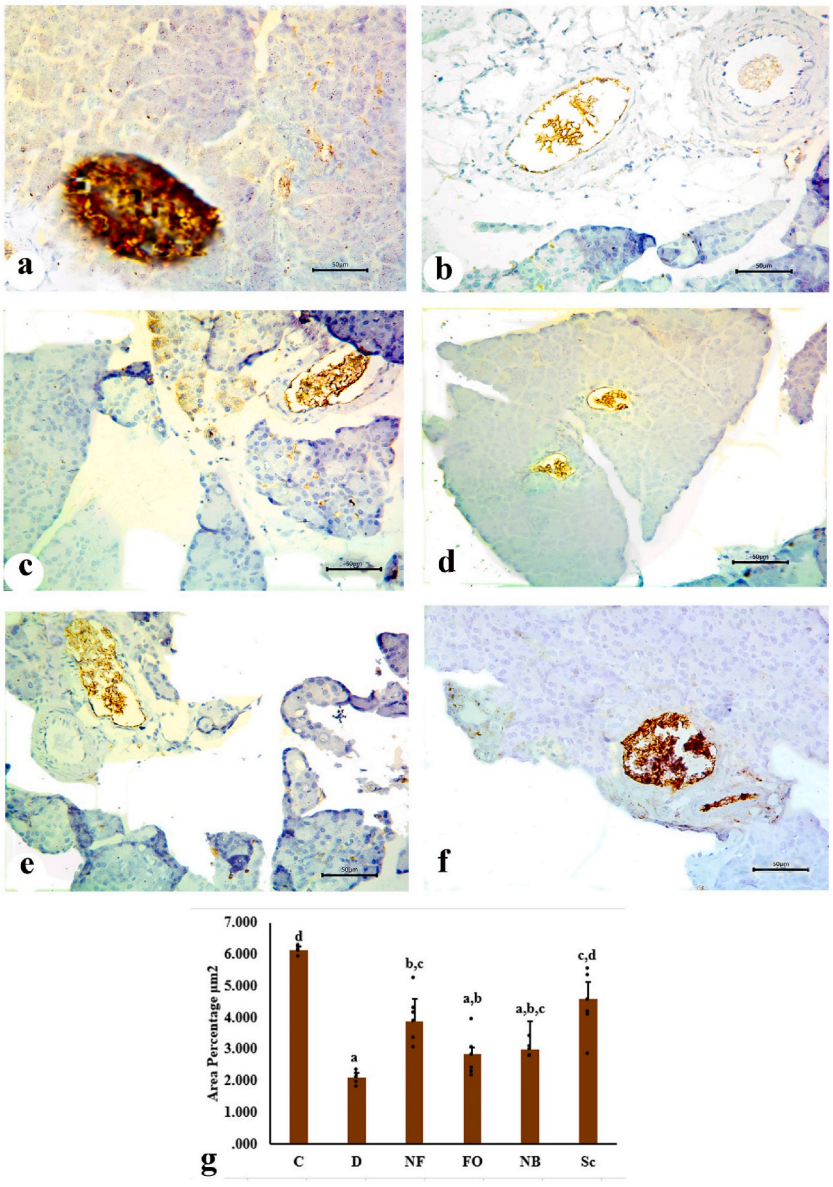

Fig. 7. Photomicrographs of the pancreatic sections showing immunohistochemical staining of insulin granules in β-cells of islets. a. Pancreatic section of the control group (C) exhibiting β-cells with strong immunoreactivity of insulin which represent most of the pancreatic islet. b. Pancreatic section of untreated diabetic group (D) revealing high reduction of insulin expression due to the severe degradation of β-cells. c. Pancreatic section of the treated group administered orally with INS-CsNBs-PD shell (F) displaying slight immunohistochemical expression of insulin related to small number of β-cells. d. Pancreatic section of treated group with free oral insulin (FO) revealing small islets with marked reduction in β-cells and immune-histochemical insulin expression as a result. e. Pancreatic section of diabetic group treated orally with CsNBs-PD shell (NB) showing noticeable decrease of insulin expression in β-cells. f. Pancreatic section of treated group injected with subcutaneous insulin (Sc) presenting increase in insulin expression relatively with regenerated β-cells. (Scale bar = 50 μm) g. Morphometric analysis is revealing changes in the mean values of area percentage of immune reactive pancreatic β-cells (μm^2), with (a, b & c) Significant compared with the control non-diabetic Group I (C), $p < 0.05$, and (b, c & d) Significant compared with the diabetic Group II (D), ($F = 7.851$, $P < 0.05$). Groups with the same superscript letter did not represent any significant differences. ($n = 6$).

In diabetic rats, both the free oral insulin-treated group (FO) and the group treated with 50 IU/kg of Cs-NBs-PD shell nano-formula had significantly reduced percentage areas of reactive islet β-cells compared to the control group I (C). Compared to the untreated diabetic group (D), the subcutaneous insulin group (Sc) (10 IU/kg) and the INS-CsNBs-PD shell oral formula group (NF) (50 IU/kg) demonstrated a significant rise in morphometric measurements (Fig. 7g).

3.5.1. Morphometric study

In diabetic rats, both the free oral insulin-treated group (FO) and the group treated with 50 IU/kg of Cs-NBs-PD shell nano-formula had significantly reduced percentage areas of reactive islet β-cells compared to the control group I (C). In comparison to the untreated diabetic group (D), the subcutaneous insulin group (Sc) (10 IU/kg) and the INS-CsNBs-PD shell oral formula group (NF) (50 IU/kg) demonstrated a significant rise in morphometric measurements (Fig. 7g).

3.6. Oxidative stress of pancreas and antioxidants

Fig. 8 (a and b) illustrate the outcomes of oxidative stress biomarkers. Diabetes significantly reduces SOD, CAT, GSH, GST, and GPx levels ($p < 0.05$). Malondialdehyde (MDA) levels significantly increase in STZ-injected animals compared to normal control rats. Treatment with orally coated forms of INS-loaded CsNBs-PD and non-coated subcutaneous insulin shows no discernible differences between them. These two treatments can reduce oxidative stress by significantly elevating SOD, CAT, GSH, GST, and GPx and lowering MDA ($p < 0.05$). The group treated with the oral CsNBs-PD shell nano-formula results in a significant reduction in MDA and an increase in antioxidants, owing to the presence of chitosan and pectin. Please correct the grammar and highlight the corrections.

3.7. Determination of serum insulin and C-peptide, IL-1β and IL-6 by ELISA assay

Fig. 9a illustrates the serum insulin and C-peptide levels in normal control and STZ-induced diabetic rats. Compared to normal rats, STZ-induced rats exhibited a significant reduction ($p < 0.05$) in serum insulin and C-peptide levels. In diabetic rats, serum levels of insulin and C-peptide were significantly elevated ($p < 0.05$) after the oral administration of the INS-CsNBs-PD shell nano-formula, similar to the effects of subcutaneous insulin. There were subsequent increases in serum insulin and C-peptide levels in the two diabetic rat groups treated with the oral CsNBs-PD shell nano-formula (NB) and free oral insulin (FO) ($p < 0.05$).

The oxidative stress-induced inflammatory response in STZ-induced diabetic rats resulted in significantly increased levels of IL-1β and IL-6 activity, according to an ELISA study of serum pro-inflammatory cytokines ($p < 0.05$). The oral treatment with the INS-CsNBs-PD shell nano-formula reestablished IL-1β and IL-6 levels to nearly normal levels compared to the normal control group. Following the injection of subcutaneous insulin and the oral administration of CsNBs-PD nanoparticles, the levels of IL-1β and IL-6 were significantly reduced compared to the STZ-diabetic group ($p < 0.05$) (Fig. 9b).

3.8. Quantitative real-time PCR

Statistical analysis revealed that the gene expression of Bax had greatly increased in diabetic rats, while the gene expression of Bcl-2, Nrf2, and HO-1 had significantly decreased ($p < 0.05$). Compared to the control group, the diabetic group and the diabetic rats administered free oral insulin both exhibited significantly higher levels of Bax mRNA expression. However, compared to the diabetic group, gene expression of Bax was significantly lower in the rat groups injected with subcutaneous insulin and in rats treated with oral nano-formulas of INS-CsNBs-PD shell and CsNBs-PD shell nanoparticles. In comparison to the diabetic group, rats administered the oral nano-formula of INS-CsNBs-PD shell NPs and CsNBs-PD shell NPs, as well as the rats treated with subcutaneous insulin injections, showed significant improvements in the gene expression of Bcl-2, Nrf2, and HO-1 ($p < 0.05$) (Fig. 10).

3.9. Western blot of NF-κB p65 and SIRT-1

To further explore the functions of NF-κB P65 and SIRT-1, we examined the effects of the INS-CsNBs-PD shell nano-formula on the expression of these proteins in STZ-induced diabetic rats. The results indicated that oral administration of the INS-CsNBs-PD shell nano-formula, as well as subcutaneous insulin, significantly increased the expression of SIRT-1 protein and decreased the expression of

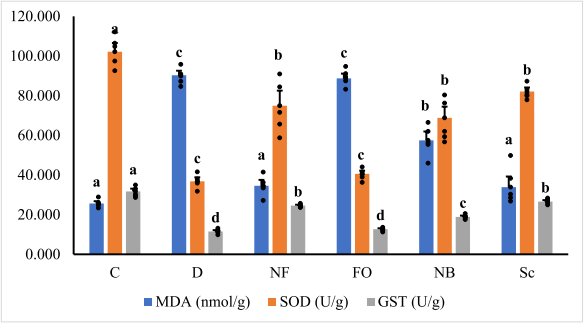

Fig. 8a. Oxidative stress biomarkers, MDA, SOD and GST in pancreatic tissue homogenate of different groups of male albino rats. Values were expressed as mean ± SE (n = 6) for each group. $^{a,b}p < 0.05$ significantly different from the diabetic group and $^{b,c,d}p < 0.05$ significantly different from the control group. Groups with the same superscript letter did not represent any significant differences. MDA ($F = 70.777$, $P < 0.05$), SOD ($F = 31.354$, $P < 0.05$), GST ($F = 99.855$, $P < 0.05$).

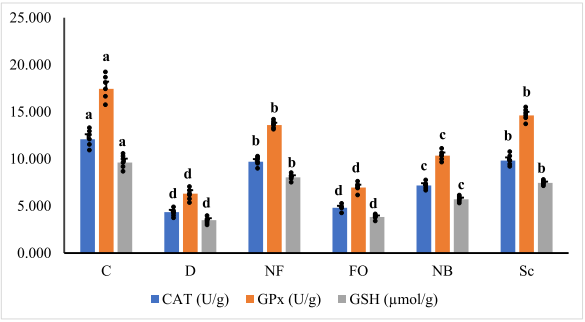

Fig. 8b. Antioxidant biomarkers, CAT, GPx and GSH in pancreatic tissue homogenate of different groups of male albino rats. Values were expressed as mean ± SE (n = 6) for each group. $^{a,b,c}p < 0.05$ significantly different from the diabetic group and $^{b,c,d}p < 0.05$ significantly different from the control group. Groups with the same superscript letter did not represent any significant differences. CAT (F = 88.426, P < 0.05), GPx (F = 104.296, P < 0.05), GSH (F = 102.769, P < 0.05).

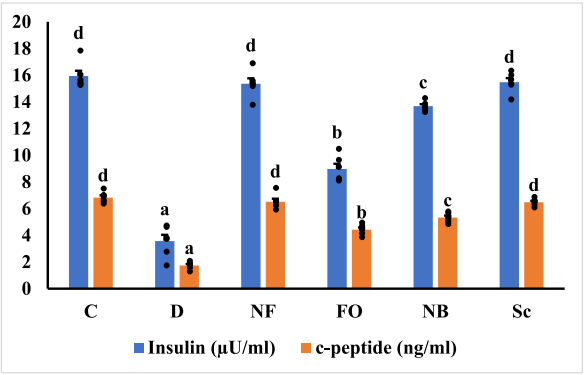

Fig. 9a. Effect of the INS-CsNBs-PD shell nano-formula on serum insulin and C-peptide in the control and experimental STZ-induced diabetic rats. Values are presented as the mean ± SE (n = 6). Comparisons are $^{b,c,d}p < 0.05$ significantly different from the diabetic group and $^{a,b,c}p < 0.05$ significantly different from the control group. Groups with the same superscript letter did not represent any significant differences. Insulin (F = 180.648, P < 0.05), C-peptide (F = 148.678, P < 0.05).

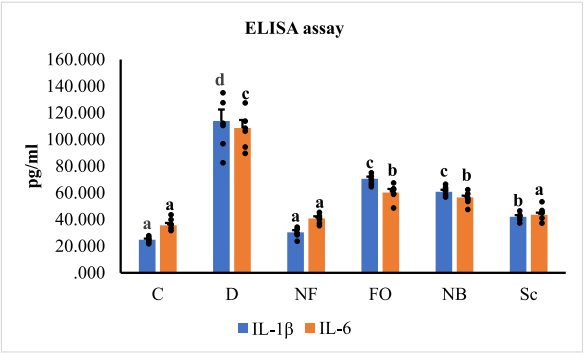

Fig. 9b. Effect of the INS-CsNBs-PD shell nano-formula on serum IL-1β and IL-6 activity in the control and STZ-induced diabetic groups. Values are presented as the mean ± SE (n = 6). Comparisons are $^{b,c,d}p < 0.05$ significantly different from the control group and $^{a,b}p < 0.05$ significantly different from the diabetic group. Groups with the same superscript letter did not represent any significant differences. IL-1β (F = 77.174, P < 0.05), IL-6 (F = 79.768, P < 0.05).

NF-κB P65 protein compared to the diabetic group ($p < 0.05$). Additionally, oral treatment with CsNBs-PD shell nanoparticles markedly enhanced SIRT-1 protein expression and reduced NF-κB P65 expression when compared to both the diabetic group and the control animals (Fig. 11).

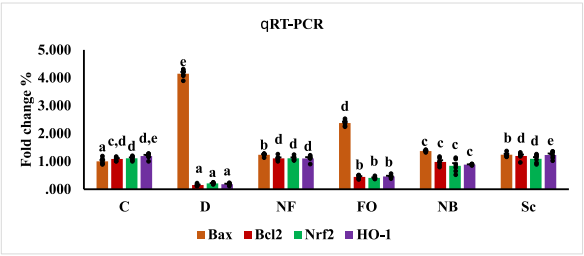

Fig. 10. Gene expression of Bax, Bcl2, Nrf2 and HO-1 in the different experimental groups. Values had statistically presented as mean ± SE ($p < 0.05$) (n = 4). $^{b,c,d}p < 0.05$ significantly different from the diabetic group and $^{b,e}p < 0.05$ significantly different from the control group. Groups with the same superscript letter did not represent any significant differences. Bax (F = 867.350, P < 0.05), Bcl2 (F = 116.987, P < 0.05), Nrf2 (F = 59.838, P < 0.05), HO-1 (F = 140.867, P < 0.05).

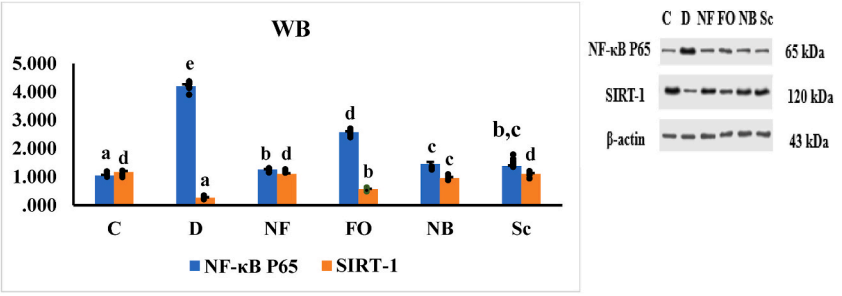

Fig. 11. Protein expression of NF-κB P65 and SIRT-1 in different experimental rat groups represented statistically by mean ± SE (n = 3) for each group. $^{b,c,d}p < 0.05$ significantly different from the diabetic group and $^{b,c}p < 0.05$ significantly different from the control group. Groups with the same superscript letter did not represent any significant differences. NF-κB P65 (F = 613.885, P < 0.05), SIRT-1 (F = 145.069, P < 0.05).

4. Discussion

This study attempts to develop an innovative oral insulin delivery method using chitosan nanobeads coated with a pectin-dextrin shell (INS-CsNBs PD shell) to manage STZ-induced diabetes in Wistar rats. The primary goal is to determine if this formula can improve blood glucose levels. It hypothesizes that the formula will enhance insulin sustained release, glucose regulation and antioxidant activity. Additionally, the research investigates its impact on pancreatic histology, specifically the preservation of beta cells. Our findings reveal that the INS-CsNBs-PD formula significantly improves blood glucose regulation, enhances histological conditions, and supports β-cell regeneration. Both oral INS-CsNBs-PD and subcutaneous insulin treatments reduce oxidative stress, elevate antioxidant enzyme levels (SOD, CAT, GSH, GST, GPx), and decrease MDA levels, with the formula showing additional benefits in reducing lipid peroxidation and increasing antioxidant activity. The treatment also increases anti-apoptotic Bcl-2 mRNA expression, decreases pro-apoptotic Bax transcription, and enhances SIRT1 protein expression, which reduces β-cell apoptosis by suppressing NF-kB. Furthermore, the formula significantly lowers proinflammatory cytokines (IL-1β and IL-6), thereby improving pancreatic islet function. These results highlight the potential of the INS-CsNBs-PD system as a non-invasive method to improve glucose regulation and protect pancreatic tissue in diabetic rats.

Discomfort, trauma, and pain are typically attributed to inadequate patient compliance with subcutaneous insulin [40]. Alternative insulin administration methods are currently being investigated. Insulin oral delivery is one of these approaches [41]. Designing nanoparticles that would preserve and improve intestinal absorption of insulin and imitate its normal rate was necessary for oral administration of insulin [42]. Chitosan nano-carriers for insulin oral delivery provide excellent drug loading, biocompatibility, muco-adhesiveness, and biodegradability, as well as drug protection from enzymatic degradation [43]. Nevertheless, chitosan nanoparticles have a history of poor stability in the stomach environment. To address this, many modified chitosan nanomaterials have been developed with improved stability and GIT absorption profiles [12]. The use of chitosan-dextrin-pectin nanoparticles for insulin delivery offers several advantages. Firstly, the nanoparticles can protect insulin from degradation in the gastrointestinal tract and enhance its absorption in the bloodstream [44]. Secondly, the mucoadhesive properties of chitosan can promote the prolonged residence of the nanoparticles in the intestine, allowing for the sustained release of insulin [45]. Finally, the use of natural polymers such as chitosan, dextrin, and pectin can minimize the toxicity and immunogenicity of the carrier system [46]. Pectin polysaccharide and pectin-based modified nano-carriers (NCs) have also been shown in several in vitro and in vivo investigations to exhibit a variety of pharmacological properties, including antidiabetic, anti-inflammatory, antioxidant, blood cholesterol regulating, antibacterial, immune system strengthening, anticancer, etc. [17]. The nanoparticle formulation applied in this study for insulin encapsulation into the core structure was consistent with the ionotropic gelation method, in line with the results of the prior experiment by Pedroso-Santana and Fleitas-Salazar, 2020 [47].

Our findings indicate that the efficiency of the intestinally absorbed coated insulin was assessed by its impact on body weight, blood glucose levels, histological and immunohistochemical alterations in the pancreas, and pancreatic oxidative biomarkers. The results of this study demonstrate the biological activity of the coated form of insulin (insulin-loaded Cs-NBs-PD shell) and its ability to cross the gastrointestinal tract (GIT) and enter the bloodstream, as demonstrated by reductions in blood glucose levels, apoptotic markers, and improvements in histopathological effects in diabetic rats administered this treatment. The supportive result obtained from the current investigation is consistent with the use of insulin-loaded modified chitosan nanoparticles to reduce blood glucose levels [48]. This improvement may be attributed to the better regulation of high blood sugar levels, which was likely due to the protection of pancreatic islets and the enhancement of insulin secretion. When free insulin is administered subcutaneously to diabetic rats, blood glucose levels drop quickly, which can result in peripheral hyperinsulinemia and diabetic microvascular complications [49]. Changes in serum insulin levels, blood sugar levels, and C-peptide, which is a byproduct of β-cell insulin, are all indicators of pancreatic function abnormalities [50]. Following oral administration of the nano-formula (INS-CsNBs-PD shell), serum insulin and C-peptide levels gradually increased. Overall, the importance of biocompatible nano-carriers and their effectiveness in delivering insulin and lowering blood glucose levels, as opposed to hyperinsulinemia brought on by subcutaneous insulin injection, suggests that uncomfortable and stressful subcutaneous injections of insulin could be replaced by the oral administration of insulin using nanoparticles in the treatment of type 1 diabetes [51].

It has been proposed that hyperglycemia promotes oxidative stress, which results in the release of pro-inflammatory cytokines [52]. Interleukin-1β (IL-1β) is a major proinflammatory cytokine that has been associated with pancreatic islet dysfunction. The pancreatic islet's ability to determine high blood glucose levels is compromised as a result of the downregulation of glucose transporter 2 (GLUT2). This prevents the production and release of insulin triggered by glucose [53]. IL-6 disrupts β-cell function and induces inflammation through interactions with monocytes and macrophages, which ultimately leads to a reduction in insulin-dependent signals [54]. Pectin polysaccharides and their nanoparticles have anti-inflammatory properties that can be improved to make anti-inflammatory medications [17]. The two primary signs of T1DM are hyperglycemia and the microscopic damage of the β-cells in the pancreatic islets of Langerhans [55]. STZ has been widely used to induce type 1 diabetes in animal models. A single intraperitoneal dose of STZ (55 mg/kg) can cause diabetes in rats [56].

In this study, STZ induced diabetes by damaging the islet's β-cells through DNA alkylation and subsequent generation of reactive oxygen species (ROS) [57]. It has been observed that oxidative stress, necrosis, and apoptosis frequently occur due to hyperglycemia and play a part in multiorgan problems in diabetes mellitus [58]. The histological results of the endocrine pancreas are in line with the current biochemical and molecular results. In diabetic rats, both the total number and quality of the insulin-producing β-cells decreased, leading to lower serum insulin levels. According to the histological evaluation, the INS-CsNBs-PD shell nano-formula, comparable to subcutaneous insulin, improved the pancreatic histological architecture. Histopathological examination showed improved degenerative changes, primarily characterized by reductions in vacuolar degenerations, necrosis, apoptosis, and congestion. Results from earlier studies support these findings, demonstrating that chitosan nanoparticles' antioxidant defense mechanism decreases lipid peroxidation, which damages organs [59].

The findings from this research imply that chitosan and pectin nanoparticles may mitigate oxidative stress by reducing lipid peroxidation. These findings imply that the protective effects of chitosan nanoparticles might be dose-dependent. In comparison to the diabetic group, diabetic rats given subcutaneous insulin and INS-CsNBs-PD shell nano-formula separately displayed a significant increase in insulin-immune positive beta-cells. Immunohistochemical examination of insulin in pancreatic tissues after subcutaneous injection of insulin to diabetic rats revealed a significant increase in β-cell immunological responsiveness, with an apparent rise in β-cell number compared to diabetic rats. In contrast, sections of the pancreas from diabetic rats given INS-CsNBs-PD shell nano-formula and CsNBs-PD shell nanoparticles both demonstrated a mild increase in β-cell reactivity and insulin-immune positive beta-cells compared to the diabetic group. Previous research revealed that chitosan nanoparticles might prevent the generation of free radicals and protect cells from oxidative stress damage [60].

It is well known that STZ can increase hyperglycemia and decrease antioxidant levels, causing oxidative stress [61]. Some of the mechanisms that could lead to oxidative stress in diabetes include the production of free radicals from glucose autoxidation, an imbalance in cellular oxidation and reduction, and a loss in enzymatic and nonenzymatic antioxidants [62]. The first line of defense against reactive oxygen species (ROS), which damage cells, is the SOD enzyme. This enzyme catalyzes the conversion of superoxide into oxygen and peroxide [63]. CAT and GPx aid in the conversion of peroxide into water. Pancreatic β-cells in diabetic rats are susceptible to oxidative stress and ultimately cell death when levels of these enzymes change [64]. The cellular membrane lipids are protected against oxidative damage by GPx, which also catalyzes the reaction of hydrogen peroxides with GSH to generate oxidized glutathione (GSSG). GST is essential for the elimination of harmful substances and their conversion into safe metabolites. In diabetic rats, the change in glutathione reductase (GR) activity is compensated for by an increase in GSSG, possibly due to the high levels of free radicals present [65]. The current study provided strong evidence that STZ induced oxidative stress due to the significant rise in MDA and a considerable decrease in SOD, GST, CAT, GPx, and GSH activities [66]. The oral administration of insulin in the form of an insulin-loaded Cs-NBs-PD shell and its influence on oxidative stress were also demonstrated by the increase in SOD, GST, CAT, GPx, and GSH activities and the reduction in MDA levels. In our study, nanobeads did not seem to cause any oxidative stress, but they were able to reduce the oxidative effects of hyperglycemia.

In fact, helper T-cell activation causes the pancreatic tissue to release inflammatory cytokines and chemokines, which lead to pancreatic degeneration and loss of insulin. In Type 1 diabetes, the anti-apoptotic molecule Bcl-2 and the pro-apoptotic molecule Bax significantly affect the apoptotic process. Apoptosis occurs when the normal balance of pro-apoptotic Bax and anti-apoptotic Bcl-2 proteins in the pancreatic β-cells is disturbed by prolonged high glucose exposure [67]. The two pathways by which apoptosis occurs are the intrinsic pathway, also known as the Bcl-2-regulated pathway or the mitochondrial pathway, which is accompanied by both

pro-apoptotic and anti-apoptotic signals, and the extrinsic pathway, also known as the death receptor-mediated pathway or the caspase pathway [68]. The current study demonstrated that downregulation of Bcl-2 gene expression and activation of the Bax genes both promoted β-cell apoptosis in diabetic rats. The INS-CsNBs-PD shell oral administration increased Bcl-2 mRNA expression, while pro-apoptotic Bax transcription levels decreased compared to STZ-induced diabetic rats. The size of the chitosan nanoparticle used in this study is anticipated to improve the efficacy of antioxidative stress and anti-apoptosis [69]. The scavenging action of chitosan is related to its capacity to donate hydrogen to free radicals, resulting in the formation of stable molecules [56]. In this study, we obviously show that the oral administration of chitosan nanoparticles to diabetic rats can reduce ROS production and increase levels of antioxidant enzymes, which in turn results in an increase in Bcl-2 expression and a decrease in Bax expression.

Our results revealed that diabetic rats exhibited markedly decreased levels of Nrf2 and HO-1 gene expression in pancreatic tissue. Nrf2 protects pancreatic β-cells against the effects of diabetes by lowering oxidative stress, controlling mitochondrial function and biogenesis, maintaining insulin content and release, and preserving β-cell mass [70]. HO-1 can decrease pancreatic damage from oxidative stress caused by elevated blood glucose levels [71]. Since Nrf2 is regarded as the main regulator of the antioxidant response, chitosan has been proven to boost Nrf2 expression, according to numerous studies [72]. The lower intracellular ROS induced by chitosan, which can increase antioxidant capacity, may be the cause of this increased Nrf2 expression in pancreatic cells [73]. More recent investigations have demonstrated that chitosan nanoparticles activate Nrf2/HO-1 [74]. This result reveals that oral administration of the INS-CsNBs-PD shell nano-formula could increase the levels of antioxidant enzymes in diabetic rats, enhancing the expression of Bcl-2, Nrf2, and HO-1 genes while decreasing the expression of the Bax gene.

The β-cell apoptosis in T1DM is significantly induced by NF-κB P65 activation [75]. In vitro and in vivo studies have shown that NF-κB P65 activation is a crucial early event in the pathobiology of diabetic complications. Inflammation, oxidative stress, and apoptosis can all be worsened by cytotoxic substances that are enhanced by activated NF-κB P65 [76]. Following oral delivery of the INS-CsNBs-PD shell nano-formula in the pancreas of diabetic rats, the current study showed a significant rise in SIRT1 protein expression. Chitosan nano-carriers with pectin could reduce the apoptosis of pancreatic β-cells by suppressing NF-κB through the activation of SIRT1 [77].

5. Conclusion

In this study, we developed a stable, functionalized INS-CsNBs-PD nano-formulation using a cost-effective method, which presents a potentially economically feasible approach. Our research provides scientific evidence supporting the potential benefits of orally administered insulin coated with chitosan-based nanomaterials in STZ-induced diabetic rats. These benefits include preventing hyperglycemia and positively influencing pancreatic β-cell activity, oxidative stress, and the gene expression of Bax, Bcl-2, Nrf2, and HO-1, as well as the protein expression of NF-κB P65 and SIRT-1. In many cases, the effects of oral INS-CsNBs-PD administration were comparable to those of subcutaneous insulin injection. Our study offers valuable insights into the potential of the INS-CsNBs-PD nano-formulation as an alternative to subcutaneous insulin. However, further investigations, including ultrastructural examinations, are necessary to understand the precise mechanisms underlying the protective effects of the INS-CsNBs-PD nano-formulation on the STZ-induced diabetic pancreas. Additionally, subsequent clinical trials in diabetic patients are recommended to validate these findings.

6. Ethics approval and consent to participate

The authors followed the ethics of research, approved, and consented to participate in this study. The Institutional Animal Care Committee of Beni-Suef University, Egypt, approved the entire conducted procedures (BSU-FS-021-128). All the authors consent and understand that their participation is voluntary and that they are free to withdraw at any time, without giving a reason and without cost. All authors understand that they will be given a copy of this consent form. All authors voluntarily agree to take part in this study.

Consent for publication

Not applicable.

Availability of data and material

The availability of raw data upon a reasonable request from the authors.

Funding

The present study was funded by the Institutional Fund Projects under grant no. IAU-DSR Project# IRB-2016-054-Sci. Therefore, authors gratefully acknowledge College of Science, Imam Abdulrahman Bin Faisal University, Dammam, Saudi Arabia.

CRediT authorship contribution statement

Hanaa Ramadan: Writing – original draft, Methodology, Formal analysis. **Nadia Moustafa:** Writing – review & editing, Supervision, Investigation. **Rasha Rashad Ahmed:** Writing – review & editing, Supervision, Conceptualization. **Ahmed A.G. El-Shahawy:** Writing – review & editing, Methodology, Investigation, Formal analysis. **Zienab E. Eldin:** Writing – review & editing, Methodology,

Formal analysis. **Suhailah S. Al-Jameel:** Writing – review & editing, Investigation, Funding acquisition. **Kamal Adel Amin:** Writing – review & editing, Project administration, Investigation. **Osama M. Ahmed:** Writing – review & editing, Resources, Investigation, Conceptualization. **Manal Abdul-Hamid:** Writing – review & editing, Supervision, Investigation, Conceptualization.

Declaration of competing interest

The authors declare the following financial interests/personal relationships which may be considered as potential competing interests:Suhailah Saud Al-Jameel reports article publishing charges was provided by Imam Abdulrahman Bin Faisal University, Dammam, Saudi Arabia. Suhailah Saud Al-Jameel reports a relationship with Imam Abdulrahman Bin Faisal University, Dammam, Saudi Arabia that includes: funding grants. Suhailah Saud Al-Jameel has patent pending to no. no conflict of interest If there are other authors, they declare that they have no known competing financial interests or personal relationships that could have appeared to influence the work reported in this paper.

Acknowledgments

The authors are thankful to Department of Chemistry, College of Science, Imam Abdulrahman Bin Faisal University, Dammam, Saudi Arabia.

Appendix A. Supplementary data

Supplementary data to this article can be found online at https://doi.org/10.1016/j.heliyon.2024.e35636.

References

[1] T. Tomita, Apoptosis of pancreatic β-cells in Type 1 diabetes, Bosn. J. Basic Med. Sci. 17 (3) (2017) 183–193.
[2] S.E. Kahn, Y.-C. Chen, N. Esser, A.J. Taylor, D.H. van Raalte, S. Zraika, C.B. Verchere, The β cell in diabetes: integrating biomarkers with functional measures, Endocr. Rev. 42 (5) (2021) 528–583.
[3] Y. Nomier, G.F. Asaad, A. Salama, M.E. Shabana, S. Alshahrani, M. Firoz Alam, T. Anwer, S. Sultana, Z. Rehman, A. Khalid, Explicit mechanistic insights of Prosopis juliflora extract in streptozotocin-induced diabetic rats at the molecular level, Saudi Pharmaceut. J. 31 (10) (2023) 101755.
[4] C.M.O. Volpe, P.H. Villar-Delfino, P.M.F. Dos Anjos, J.A. Nogueira-Machado, Cellular death, reactive oxygen species (ROS) and diabetic complications, Cell Death Dis. 9 (2) (2018) 119.
[5] M. Anděl, V. Němcová, N. Pavlíková, J. Urbanová, M. Cecháková, A. Havlová, R. Straková, L. Večeřová, V. Mandys, J. Kovář, P. Heneberg, J. Trnka, J. Polák, [Factors causing damage and destruction of beta-cells of the islets of Langerhans in the pancreas], Vnitr. Lek. 60 (9) (2014) 684–690.
[6] M.K. Prasad, S. Mohandas, K.M. Ramkumar, Dysfunctions, molecular mechanisms, and therapeutic strategies of pancreatic β-cells in diabetes, Apoptosis 28 (7–8) (2023) 958–976.
[7] K.N. Keane, V.F. Cruzat, R. Carlessi, P.I. de Bittencourt Jr., P. Newsholme, Molecular events linking oxidative stress and inflammation to insulin resistance and β-cell dysfunction, Oxid. Med. Cell. Longev. 2015 (2015) 181643.
[8] E. Casper, The crosstalk between Nrf2 and NF-κB pathways in coronary artery disease: can it be regulated by SIRT6? Life Sci. 330 (2023) 122007.
[9] H. Iskender, E. Dokumacioglu, T.M. Sen, I. Ince, Y. Kanbay, S. Saral, The effect of hesperidin and quercetin on oxidative stress, NF-κB and SIRT1 levels in a STZ-induced experimental diabetes model, Biomed. Pharmacother. 90 (2017) 500–508.
[10] P. Newsholme, K.N. Keane, R. Carlessi, V. Cruzat, Oxidative stress pathways in pancreatic β-cells and insulin-sensitive cells and tissues: importance to cell metabolism, function, and dysfunction, Am. J. Physiol. Cell Physiol. 317 (3) (2019) C420–C433.
[11] V. Pathak, N.M. Pathak, C.L. O'neill, J. Guduric-Fuchs, R.J. Medina, Therapies for type 1 diabetes: current scenario and future perspectives, Clin. Med. Insights Endocrinol. Diabetes 12 (2019) 1179551419844521.
[12] M. Wang, C. Wang, S. Ren, J. Pan, Y. Wang, Y. Shen, Z. Zeng, H. Cui, X. Zhao, Versatile oral insulin delivery nanosystems: from materials to nanostructures, Int. J. Mol. Sci. 23 (6) (2022) 3362.
[13] A. Abdel-Moneim, H. Ramadan, Novel strategies to oral delivery of insulin: current progress of nanocarriers for diabetes management, Drug Dev. Res. 83 (2) (2022) 301–316.
[14] V. Mikušová, P. Mikuš, Advances in chitosan-based nanoparticles for drug delivery, Int. J. Mol. Sci. 22 (17) (2021) 9652.
[15] E.B. Souto, S.B. Souto, J.R. Campos, P. Severino, T.N. Pashirova, L.Y. Zakharova, A.M. Silva, A. Durazzo, M. Lucarini, A.A. Izzo, A. Santini, Nanoparticle delivery systems in the treatment of diabetes complications, Molecules 24 (23) (2019) 4209.
[16] S.T. Minzanova, V.F. Mironov, D.M. Arkhipova, A.V. Khabibullina, L.G. Mironova, Y.M. Zakirova, V.A. Milyukov, Biological activity and pharmacological application of pectic polysaccharides: a review, Polymers 10 (12) (2018) 1407.
[17] W.M. Kedir, E.M. Deresa, T.F. Diriba, Pharmaceutical and drug delivery applications of pectin and its modified nanocomposites, Heliyon 8 (9) (2022) e10654.
[18] Q. Hu, Y. Lu, Y. Luo, Recent advances in dextran-based drug delivery systems: from fabrication strategies to applications, Carbohydr. Polym. 264 (2021) 117999.
[19] S. Seyam, N.A. Nordin, M. Alfatama, Recent progress of chitosan and chitosan derivatives-based nanoparticles: pharmaceutical perspectives of oral insulin delivery, Pharmaceuticals 13 (10) (2020) 307.
[20] S. Padugupati, S. Ramamoorthy, K. Thangavelu, D. Sarma, D. Jamadar, Effective dose of streptozotocin to induce diabetes mellitus and variation of biophysical and biochemical parameters in albino wistar rats, J. Clin. Diagn. Res. 15 (10) (2021) 1–5.
[21] C. Damgé, P. Maincent, N. Ubrich, Oral delivery of insulin associated to polymeric nanoparticles in diabetic rats, J. Contr. Release 117 (2) (2007) 163–170.
[22] Y. Wang, H. Sun, J. Zhang, Z. Xia, W. Chen, Streptozotocin-induced diabetic cardiomyopathy in rats: ameliorative effect of PIPERINE via Bcl2, Bax/Bcl2, and caspase-3 pathways, Biosci. Biotechnol. Biochem. 84 (12) (2020) 2533–2544.
[23] N.J. Kruger, The Bradford method for protein quantitation, Methods Mol. Biol. 32 (1994) 9–15.
[24] A. Ahangarpour, A.A. Oroojan, L. Khorsandi, M. Kouchak, M. Badavi, Solid lipid nanoparticles of myricitrin have antioxidant and antidiabetic effects on streptozotocin-nicotinamide-induced diabetic model and myotube cell of male mouse, Oxid. Med. Cell. Longev. 2018 (2018) 7496936.
[25] M.C. Sabu, R. Kuttan, Antidiabetic activity of Aegle marmelos and its relationship with its antioxidant properties, Indian J. Physiol. Pharmacol. 48 (1) (2004) 81–88.

[26] O.O. Erejuwa, S.A. Sulaiman, M.S. Wahab, S.K. Salam, M.S. Salleh, S. Gurtu, Antioxidant protective effect of glibenclamide and metformin in combination with honey in pancreas of streptozotocin-induced diabetic rats, Int. J. Mol. Sci. 11 (5) (2010) 2056–2066.
[27] J.D. Bancroft, M. Gamble, in: Theory and Practice of Histological Techniques 5th, Edinburgh. Churchill Livingstone Pub, 2002, pp. 172–175, 593-175, Am J Cancer Prev. 3(6) (2015) 122-175.
[28] S.C. Campbell, W.M. Macfarlane, Detection of insulin production by immunohistochemistry, Methods Mol. Med. 83 (2003) 47–49.
[29] C.A. Schneider, W.S. Rasband, K.W. Eliceiri, NIH Image to ImageJ: 25 years of image analysis, Nat. Methods 9 (2012) 671–675.
[30] D.R.I. Abdel-Gawad, W.A. Moselhy, R.R. Ahmed, H.M. Al-Muzafar, K.A. Amin, M.M. Amin, E.S. Nahass, K.A.H. Abdou, Therapeutic effect of mesenchymal stem cells on histopathological, immunohistochemical, and molecular analysis in second-grade burn model, Stem Cell Res. Ther. 12 (1) (2021) 308.
[31] J.W. Hwang, S.-N. Kim, N. Myung, D. Song, G. Han, G.-U. Bae, M.T. Bedford, Y.K. Kim, PRMT5 promotes DNA repair through methylation of 53BP1 and is regulated by Src-mediated phosphorylation, Commun. Biol. 3 (1) (2020) 428.
[32] X. Rao, X. Huang, Z. Zhou, X. Lin, An improvement of the 2ˆ(-delta delta CT) method for quantitative real-time polymerase chain reaction data analysis, Biostat Bioinforma Biomath 3 (3) (2013) 71–85.
[33] L.S. Binmahfouz, B.G. Eid, A.M. Bagher, R.A. Shaik, N.S. Binmahfouz, A.B. Abdel-Naim, Piceatannol SNEDDS attenuates estradiol-induced endometrial hyperplasia in rats by modulation of NF-κB and Nrf2/HO-1 axes, Nutrients 14 (9) (2022) 1891.
[34] H. Almukadi, B.G. Eid, R.A. Shaik, A.B. Abdel-Naim, A. Esmat, Auraptene nanoparticles ameliorate testosterone-induced benign prostatic hyperplasia in rats: emphasis on antioxidant, anti-inflammatory, proapoptotic and PPARs activation effects, Biomed. Pharmacother. 143 (2021) 112199.
[35] A.R. Ayob, A.H. Al-Najjar, A.S. Awad, Amelioration of bile duct ligation induced liver injury by lactoferrin: role of Nrf2/HO-1 pathway, AIJPMS 2 (2021) 84–90.
[36] A. Bagalagel, R. Diri, A. Noor, D. Almasri, H.T. Bakhsh, H.I. Kutbi, M.M.H. Al-Gayyar, Curative effects of fucoidan on acetic acid induced ulcerative colitis in rats via modulating aryl hydrocarbon receptor and phosphodiesterase-4, BMC Complement Med Ther 22 (1) (2022) 1–12.
[37] C.A. Kelm-Nelson, S.A. Stevenson, M.R. Ciucci, Data in support of qPCR primer design and verification in a Pink1 -/- rat model of Parkinson disease, Data Brief 8 (2016) 360–363.
[38] B.F. Brian, C.R. Guerrero, T.S. Freedman, Immunopharmacology and quantitative analysis of tyrosine kinase signaling, Curr. Protoc. Im. 130 (1) (2020) e104.
[39] T. Mahmood, P.C. Yang, Western blot: technique, theory, and trouble shooting, N. Am. J. Med. Sci. 4 (9) (2012) 429–434.
[40] T.A. Debele, Y. Park, Application of nanoparticles: diagnosis, therapeutics, and delivery of insulin/anti-diabetic drugs to enhance the therapeutic efficacy of diabetes mellitus, Life 12 (12) (2022) 2078.
[41] S. Karmakar, M. Bhowmik, B. Laha, S. Manna, Recent advancements on novel approaches of insulin delivery, Med Nov Technol Devices. 19 (2023) 100253.
[42] A.B. Meneguin, A.L.P. Silvestre, L. Sposito, M.P.C. de Souza, R.M. Sábio, V.H.S. Araújo, B.S.F. Cury, M. Chorilli, The role of polysaccharides from natural resources to design oral insulin micro- and nanoparticles intended for the treatment of Diabetes mellitus: a review, Carbohydr. Polym. 256 (2021) 117504.
[43] A. Patel, M. Patel, X. Yang, A.K. Mitra, Recent advances in protein and peptide drug delivery: a special emphasis on polymeric nanoparticles, Protein Pept. Lett. 21 (11) (2014) 1102–1120.
[44] A. Qiu, Y. Wang, G. Zhang, H. Wang, Natural polysaccharide-based nanodrug delivery systems for treatment of diabetes, Polymers 14 (15) (2022) 3217.
[45] E.M.A. Hejjaji, A.M. Smith, G.A. Morris, Evaluation of the mucoadhesive properties of chitosan nanoparticles prepared using different chitosan to tripolyphosphate (CS: TPP) ratios, Int. J. Biol. Macromol. 120 (Pt B) (2018) 1610–1617.
[46] P. Prasher, M. Sharma, M. Mehta, S. Satija, A.A. Aljabali, M.M. Tambuwala, K. Anand, N. Sharma, H. Dureja, N.K. Jha, G. Gupta, M. Gulati, S.K. Singh, D. K. Chellappan, K.R. Paudel, P.M. Hansbro, K. Dua, Current-status and applications of polysaccharides in drug delivery systems, Colloids Interface Sci Commun 42 (2021) 100418.
[47] S. Pedroso-Santana, N. Fleitas-Salazar, Ionotropic gelation method in the synthesis of nanoparticles/microparticles for biomedical purposes, Polym. Int. 69 (2020) 443–447.
[48] G. Revathi, S. Elavarasi, K. Saravanan, M. Ashokkumar, C. Egbuna, Greater efficiency of polyherbal drug encapsulated biosynthesized chitosan nano-biopolymer on diabetes and its complications, Int. J. Biol. Macromol. 240 (2023) 124445.
[49] H.A. Asal, K.R. Shoueir, M.A. El-Hagrasy, E.A. Toson, Controlled synthesis of in-situ gold nanoparticles onto chitosan functionalized PLGA nanoparticles for oral insulin delivery, Int. J. Biol. Macromol. 209 (Pt B) (2022) 2188–2196.
[50] O.M. Ahmed, A.S. Saleh, E.A. Ahmed, M.M. Ghoneim, H.A. Ebrahim, M.A. Abdelgawad, M. Abdel-Gabbar, Efficiency of bone marrow-derived mesenchymal stem cells and hesperetin in the treatment of streptozotocin-induced type 1 diabetes in wistar rats, Pharmaceuticals 16 (6) (2023) 859.
[51] E.L. Vasconcelos Silva, A.C.J. Oliveira, L.M.C.C. Moreira, E.C. Silva-Filho, A.G. Wanderley, M.F.R. Soares, J.L. Soares-Sobrinho, Insulin-loaded nanoparticles based on acetylated cashew gum/chitosan complexes for oral administration and diabetes treatment, Int. J. Biol. Macromol. 242 (Pt 1) (2023) 124737.
[52] F. Bulut, M. Adam, A. Özgen, M.G. Hekim, S. Ozcan, S. Canpolat, M. Ozcan, Protective effects of chronic humanin treatment in mice with diabetic encephalopathy: a focus on oxidative stress, inflammation, and apoptosis, Behav. Brain Res. 452 (2023) 114584.
[53] A. Godfrey, N. Aisharwya, B. Babiker, D. Gitima, Role of interleukin-1β in pancreatic islet cells dysfunction and apoptosis in pancreatic islet transplantation, Res. J. Pharm. Technol. 13 (8) (2020) 3947–3951.
[54] Z. Jing, Y. Li, Y. Ma, X. Zhang, X. Liang, X. Zhang, Leverage biomaterials to modulate immunity for type 1 diabetes, Front. Immunol. 13 (2022) 997287.
[55] N.F. Abo El-Magd, N.M. Ramadan, S.M. Eraky, The ameliorative effect of bromelain on STZ-induced type 1 diabetes in rats through Oxi-LDL/LPA/LPAR1 pathway, Life Sci. 285 (2021) 119982.
[56] G. Wardani, J. Nugraha, M.R. Mustafa, R. Kurnijasanti, S.A. Sudjarwo, Antioxidative stress and antiapoptosis effect of chitosan nanoparticles to protect cardiac cell damage on streptozotocin-induced diabetic rat, Oxid. Med. Cell. Longev. 2022 (2022) 3081397.
[57] A.V. Lugovaya, N.M. Kalinina, V.P. Mitreikin, Y.V. Emanuel, Y.P. Kovalchuk, A.V. Artyomova, Spontaneous and activation-induced apoptosis of peripheral blood mononuclear cells in the pathogenesis of type 1 diabetes mellitus, Med. Immunol. 22 (1) (2019) 123–134. .
[58] E.G. Novoselova, O.V. Glushkova, M.O. Khrenov, S.M. Lunin, T.V. Novoselova, S.B. Parfenuyk, Role of innate immunity and oxidative stress in the development of type 1 diabetes mellitus, peroxiredoxin 6 as a new anti-diabetic agent, Biochemistry 86 (12) (2021) 1579–1589.
[59] G. Kalantarian, N. Ziamajidi, R. Abbasalipourkabir, R. Mahjub, M.T. Goodarzi, M. Saidijam, S. Soleimani Asl, M. Jamshidi, Effect of insulin-loaded trimethyl chitosan nanoparticles on genes expression in the hippocampus of diabetic rats, J. Basic Clin. Physiol. Pharmacol. 31 (2) (2019) 2019–20147.
[60] E.M. Shaaban, K.S. Amr, A.M. Mohamadin, D.E. Ellakwa, The effect of insulin loaded nanoparticles on immuno-reactivity of beta cells in rats with diabetes type 1, AIJPMS 3 (1) (2023) 96–104.
[61] N.J. Byrne, N.S. Rajasekaran, E.D. Abel, H. Bugger, Therapeutic potential of targeting oxidative stress in diabetic cardiomyopathy, Free Radic. Biol. Med. 169 (2021) 317–342.
[62] C.M. Curieses Andrés, J.M. Pérez De La Lastra, C. Andrés Juan, F.J. Plou, E. Pérez-Lebeña, From reactive species to disease development: effect of oxidants and antioxidants on the cellular biomarkers, J. Biochem. Mol. Toxicol. 37 (11) (2023) e23455.
[63] A.A. Adwas, A. Elsayed, A.E. Azab, F.A. Quwaydir, Oxidative stress and antioxidant mechanisms in human body, J Appl Biotechnol Bioeng. 6 (1) (2019) 43–47.
[64] F.M. El-Demerdash, Y. Talaat, N.F. Ghanem, W. Kang, Actinidia deliciosa mitigates oxidative stress and changes in pancreatic α-, β-, and δ-cells and immunohistochemical and histological architecture in diabetic rats, Evid Based Complement Alternat Med 2022 (2022) 5224207.
[65] V.E. Sarmiento-Ortega, D. Moroni-González, A. Diaz, E. Brambila, S. Treviño, ROS and ERK pathway mechanistic approach on hepatic insulin resistance after chronic oral exposure to cadmium NOAEL dose, Biol. Trace Elem. Res. 201 (8) (2023) 3903–3918.
[66] S. Chupradit, D. Bokov, M.Y. Zamanian, M. Heidari, E. Hakimizadeh, Hepatoprotective and therapeutic effects of resveratrol: a focus on anti-inflammatory and antioxidative activities, Fundam. Clin. Pharmacol. 36 (3) (2022) 468–485.
[67] R. Naderi, A. Shirpoor, M. Samadi, B. Pourheydar, A. Moslehi, Tropisetron attenuates pancreas apoptosis in the STZ-induced diabetic rats: involvement of SIRT1/NF-κB signaling, Pharmacol. Rep. 72 (6) (2020) 1657–1665.
[68] L. Lossi, The concept of intrinsic versus extrinsic apoptosis, Biochem. J. 479 (3) (2022) 357–384.
[69] Y. Wang, C. Wang, K. Li, X. Song, X. Yan, L. Yu, Z. He, Recent advances of nanomedicine-based strategies in diabetes and complications management: diagnostics, monitoring, and therapeutics, J. Contr. Release 330 (2021) 618–640.

[70] N. Eguchi, N.D. Vaziri, D.C. Dafoe, H. Ichii, The role of oxidative stress in pancreatic β cell dysfunction in diabetes, Int. J. Mol. Sci. 22 (4) (2021) 1509.
[71] V. Sorrenti, M. Raffaele, L. Vanella, R. Acquaviva, L. Salerno, V. Pittalà, S. Intagliata, C. Di Giacomo, Protective effects of caffeic acid phenethyl ester (CAPE) and novel cape analogue as inducers of heme oxygenase-1 in streptozotocin-induced type 1 diabetic rats, Int. J. Mol. Sci. 20 (10) (2019) 2441.
[72] S.H. Shahcheraghi, F. Salemi, N. Peirovi, J. Ayatollahi, W. Alam, H. Khan, L. Saso, Nrf2 regulation by curcumin: molecular aspects for therapeutic prospects, Molecules 27 (1) (2022) 167.
[73] Q.-X. Mei, J.-H. Hu, Z.-H. Huang, J.-J. Fan, C.-L. Huang, Y.-Y. Lu, X.-P. Wang, Y. Zeng, Pretreatment with chitosan oligosaccharides attenuate experimental severe acute pancreatitis via inhibiting oxidative stress and modulating intestinal homeostasis, Acta Pharmacol. Sin. 42 (6) (2021) 942–953.
[74] E. Mo, Y.A. Ebedy, M.A. Ibrahim, K.Y. Farroh, E.I. Hassanen, Newly synthesized chitosan-nanoparticles attenuate carbendazim hepatorenal toxicity in rats via activation of Nrf2/HO1 signalling pathway, Sci. Rep. 12 (1) (2022) 9986.
[75] S. Dinić, J. Arambašić Jovanović, A. Uskoković, M. Mihailović, N. Grdović, A. Tolić, J. Rajić, M. Đorđević, M. Vidaković, Oxidative stress-mediated beta cell death and dysfunction as a target for diabetes management, Front. Endocrinol. 13 (2022) 1006376.
[76] Q. Kang, C. Yang, Oxidative stress and diabetic retinopathy: molecular mechanisms, pathogenetic role and therapeutic implications, Redox Biol. 37 (2020) 101799.
[77] V. Gowd, Kanika, C. Jori, A.A. Chaudhary, H.A. Rudayni, S. Rashid, R. Khan, Resveratrol and resveratrol nano-delivery systems in the treatment of inflammatory bowel disease, J. Nutr. Biochem. 109 (2022) 109101.